

Oxygen Annealing of $\text{GdBa}_2\text{Cu}_3\text{O}_{7-\delta}$ Superconducting Thin Films: Influence of Annealing Time

Ruslan Popov , Jens Hänisch , and Bernhard Holzapfel 

Abstract— $\text{GdBa}_2\text{Cu}_3\text{O}_{7-\delta}$ (GdBCO) superconducting thin films, grown by Pulsed Laser Deposition (PLD) on $\text{MgO}(100)$ single crystals are oxygen annealed using two different approaches: *in-situ* (oxygen annealing in PLD chamber) and *ex-situ* (oxygen annealing in tubular furnace). Their structural and transport properties are investigated in relation to annealing time (t_{ann}) at 450 °C. *In-situ* annealed GdBCO thin films require at least 15 min of annealing to achieve high in-field critical current densities (J_c), while *ex-situ* annealed samples achieve high in-field J_c already after 5 min of oxygen annealing at 450 °C and 1 bar of oxygen pressure.

Index Terms—GdBCO, oxygen annealing, pulsed laser deposition, thin films.

I. INTRODUCTION

$\text{REBa}_2\text{Cu}_3\text{O}_{7-\delta}$ (REBCO, RE=Rare Earth) is one of the promising superconducting material classes with a great potential to revolutionize many aspects of modern society. In recent years, coated conductors (CC) containing a REBCO superconducting layer were successfully demonstrated to significantly improve characteristics in large scale applications such as motors, generators, cables and magnets, and moreover, to reduce the amount of material and infrastructure needed. Nevertheless, despite of numerous advantages, many issues remain both during production of such technologies and in the materials part of REBCO-based superconductors.

Flux lines interact with defects present in the REBCO matrix, which defines the critical current density (J_c). Therefore, for further enhancement of transport properties and characteristics of technologies based on high temperature superconductors, it is necessary to understand what type of defects is efficient for flux pinning, what concentration of defects is the optimum and how are they affected by the preparation parameters of REBCO-based superconducting thin films.

In a recent study J. P. F. Feighan et al. [1] have shown that various applications imply different temperature and magnetic field operation regimes and, thus, the pinning morphologies have to be readjusted accordingly. Since it was shown by Y. Yamada et al. [2] and A. Goyal et al. [3] that secondary phases can form

columnar defects in REBCO-based superconducting thin films and that these defects can result in 2–5 fold increase of J_c [3], [4], the main strategy of improving transport properties has been the introduction of such secondary phases in various amounts. Additionally, in pristine REBCO thin films and the ones with artificial pinning centers (APC), deposition parameters such as substrate temperature (T_{sub}) and deposition rate (v_{dep}) [5], [6], [7] control the defect morphology and final J_c . However, every REBCO thin film preparation method includes oxygen annealing, which may be considered as one of the most important steps since it is required to introduce additional atoms of oxygen to create the superconducting phase.

Over the last decades, various aspects of oxygen annealing such as oxygen diffusion in single crystals and thin films [8], [9], [10], [11], dependence of the diffusion coefficient on temperature and its anisotropy [12], [13], [14], [15], [16], and correlation between oxygen content and critical temperature [17], [18], [19] have been thoroughly investigated. However, no correlations among oxygen annealing, the resulting defect morphology, and, thus, the transport properties have been established yet. Therefore, in a series of studies we are going to shed light on this issue. This work focuses on the influence of the annealing time (t_{ann}).

II. EXPERIMENTAL PROCEDURES

Thin film deposition: Pristine $\text{GdBa}_2\text{Cu}_3\text{O}_{7-\delta}$ films have been grown on $\text{MgO}(100)$ single crystals by pulsed laser deposition (PLD) using a 3rd harmonic ($\lambda = 355$ nm) Nd:YAG laser. Laser pulses of 80 mJ were focused onto a spot of 2 mm diameter to achieve 2.5 J cm^{-2} laser fluence. 6000 pulses have been used for each sample to obtain 220–250 nm thick films. The optimum growth conditions in such experimental setup have been found to be $T_{\text{sub}} = 800$ °C, $f = 10$ Hz and $p\text{O}_2 = 0.4$ mbar.

Oxygen annealing: To study the influence of the oxygen annealing time, two approaches have been implemented. For *in-situ* annealing (in the PLD chamber), after the deposition all films were cooled to 450 °C in 0.4 mbar oxygen and the samples were annealed at 450 °C and 0.4 bar. The annealing time (t_{ann}) was varied between 5 and 60 min. For *ex-situ* annealing (in a tubular furnace), the films were cooled to room temperature (RT) in 0.4 mbar oxygen in the PLD chamber. Afterwards, they were placed in the tubular furnace, where they were heated to 800 °C in argon atmosphere, cooled to 450 °C in a mixture of oxygen and argon and then annealed at 450 °C and 1 bar of oxygen with a flow of 2 L/min.

Characterization: Phase purity and microstructure of the GdBCO thin films were investigated by X-ray diffractometry

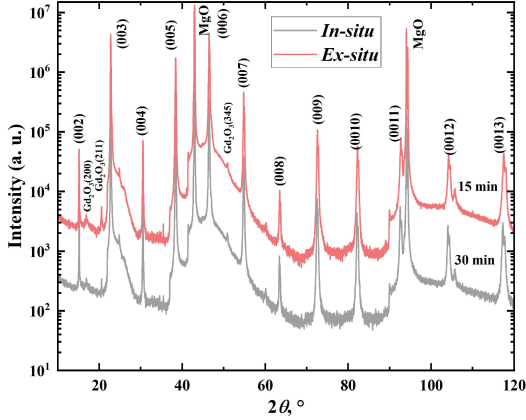


Fig. 1. θ - 2θ scans of *in-situ* annealed GdBCO thin film at $t_{\text{ann}} = 30$ min and *ex-situ* annealed GdBCO thin film at $t_{\text{ann}} = 15$ min.

TABLE I

BASIC SUPERCONDUCTING AND STRUCTURAL PROPERTIES OF *IN-SITU* AND *EX-SITU* ANNEALED GdBCO THIN FILMS

<i>in-situ</i> , t_{ann} , min	<i>ex-situ</i> , t_{ann} , min	T_c , K	<i>c</i> -axis, nm
5		71.8	1.175
15		84.4	1.174
30		92.7	1.173
60		91.9	1.172
	5	93.4	1.172
	15	93.3	1.172
	30	93.1	1.172
	60	93.2	1.172

(XRD) using a Bruker D8 with Cu K_α radiation. After initial characterization, the films were patterned into 1 mm long and 40–50 μm wide bridges using photolithography and wet-chemical etching with subsequent gold contacts deposition for transport property measurements. Critical temperatures (T_c), field dependence of the critical current density (J_c) and its dependence on the orientation of magnetic field have been measured resistively using four-probe method on a Physical Properties Measurement System with magnetic fields up to 14 T. A criterion of $R(T)/R(100 \text{ K}) \approx 10^{-7}$ was used to define T_c and $1 \mu\text{V}/\text{cm}$ for calculating J_c .

III. RESULTS

θ - 2θ XRD patterns of *in-situ* and *ex-situ* annealed GdBCO thin films (Fig. 1) show (00l) reflections of GdBCO and (200) and (345) reflections of Gd₂O₃. Compared to *in-situ*, *ex-situ* annealed GdBCO thin films have an additional (211) reflection of Gd₂O₃. T_c and *c*-axis lattice parameters of *in-situ* annealed GdBCO thin films (Table I) show that, except the sample annealed for 5 min, all GdBCO thin films exhibit insignificant changes of the *c*-axis lattice parameter and have an optimum oxygen content compared to literature [20]. The behavior of T_c does not follow the same pattern. The maximum of 92.7 K is reached for $t_{\text{ann}} = 30$ min, while T_c for $t_{\text{ann}} = 5$ min and 15 min are harshly reduced.

Field dependence of J_c of *in-situ* annealed GdBCO thin films (Fig. 2) shows that, similar to the situation of T_c , the highest in-field and self-field $J_c(0 \text{ T}, 77 \text{ K}) = 3.2 \text{ MAcm}^{-2}$ are achieved for the sample annealed for 30 min. The sample annealed for 5 min has a T_c below 77 K, thus, no J_c is measured. The sample annealed for 15 min has the strongest dependence on magnetic fields at 77 K. At 10 K the trends are similar with the exception that J_c for the sample annealed for 5 min is

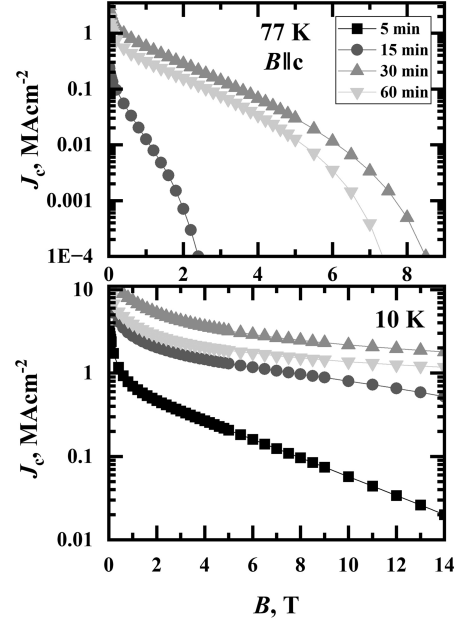


Fig. 2. Field dependence of J_c of *in-situ* annealed GdBCO thin films.

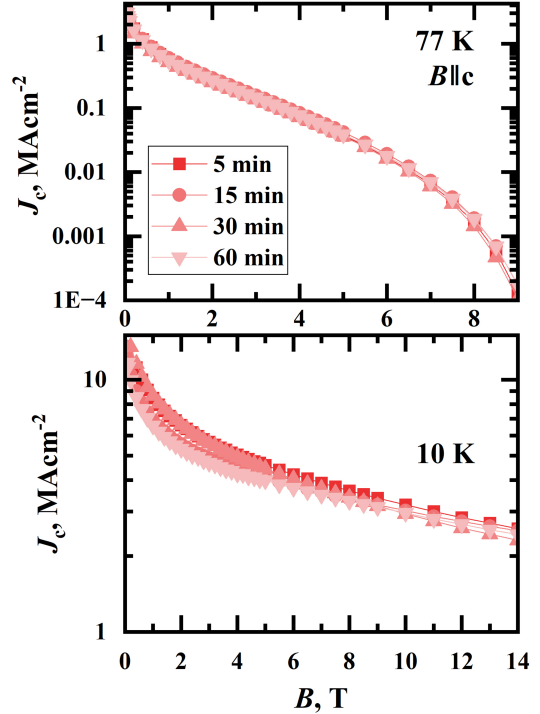


Fig. 3. Field dependence of J_c of *ex-situ* annealed GdBCO thin films.

now detectable and shows the strongest dependence on the magnetic fields. Compared to *in-situ*, *ex-situ* annealed GdBCO thin films do not show drastic changes, neither at 77 K nor at 10 K (see Fig. 3). However, the sample annealed for 15 min exhibits slightly higher in-field J_c compared to the other samples. All *ex-situ* annealed GdBCO thin films exhibit somewhat similar self-field J_c equal to $J_c(0 \text{ T}, 77 \text{ K}) = 3.7 \text{ MAcm}^{-2}$. Self-field J_c achieved for both oxygen annealing approaches fall well into the range that was previously reported for pristine REBCO based superconducting thin films [7], [20]. Additionally, comparing high field J_c for *in-situ* and *ex-situ* annealed samples, one may

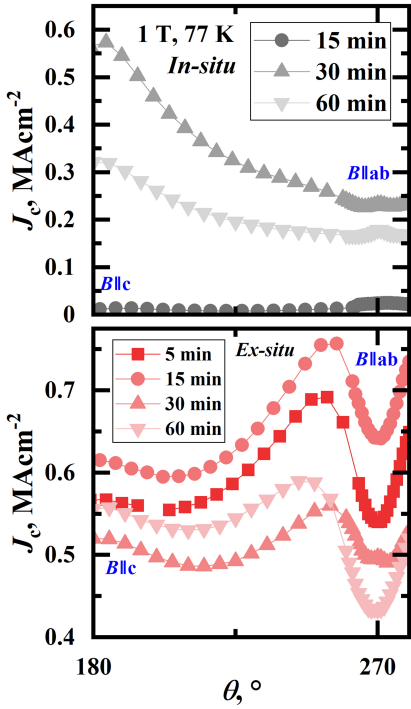


Fig. 4. $J_c(\theta)$ characteristics of *in-situ* and *ex-situ* annealed GdBCO thin films at 1 T and 77 K.

notice that by changing the oxygen annealing procedure, it is possible to increase J_c drastically.

The dependence of J_c on magnetic field orientation (Fig. 4), shows a large peak in *c*-direction, a peak in *ab*-direction, and barely visible shoulders for *in-situ* annealed GdBCO thin films for 30 min. The sample annealed for 15 min exhibits a nearly flat area around the *c*-direction with barely visible peak in *ab*-direction. Compared to *in-situ*, *ex-situ* annealed GdBCO thin films possess similar shapes of the anisotropy behavior. *Ex-situ* annealed GdBCO thin films are characterized by a peak in *c*-axis direction, a dip around the *ab*-direction and a large shoulder between 235° and 270°.

IV. DISCUSSION

The presence of an additional (211) reflection of Gd₂O₃ for the *ex-situ* annealed samples on Fig. 1 indicates that heating to 800 °C in argon leads to a partial decomposition of Gd123 into Gd₂O₃, Gd163 and liquid phases, according to the phase stability diagram proposed by J.-W. Lee et al. [21]. This induces the formation of additional Gd₂O₃ nanoparticles (NPs).

The harsh reduction of T_c for *in-situ* annealed GdBCO thin films, while *c*-axis lattice parameters remain nearly constant, may be attributed to strain effects, which are possibly caused by large defects such as stacking faults (SF) and Gd-oxide NPs. Comparison of *c*-axis lattice parameters and T_c shows that *in-situ* and *ex-situ* oxygen annealing approaches possibly have different oxygen activation rates, according to P. Cayado et al. [22]. Additionally, one may assume different oxygen in-diffusion rates for both approaches. The diffusion coefficient depends on the concentration of oxygen, which in the tubular furnace is continuously supplied, while in the PLD chamber it remains constant. Another important feature that may be affecting the final structural and superconducting properties is the presence of additional oxygen in- and out-diffusion steps for *ex-situ* annealed

GdBCO thin films. According to previous studies on YBCO thin films [11], introduction of additional steps results in a faster oxygen intake.

Similar to the strong reduction of T_c for $t_{\text{ann}} = 5$ and 15 min, self-field and in-field J_c of *in-situ* annealed GdBCO thin films vary significantly over t_{ann} . In addition to the features mentioned above, it is possible that in case of oxygen annealing in the PLD chamber a temperature gradient is present as well, which may affect the superconducting properties. In the PLD chamber, 450 °C is kept on the heater itself, while the surroundings have a temperature gradient. Considering the dependence of the diffusion coefficient on temperature and concentration of oxygen molecules, the oxygen intake during *in-situ* oxygen annealing may be much slower. Compared to the *in-situ* case, during annealing in the tubular furnace oxygen is permanently supplied. Moreover, an insulation and all-side heating in the tubular furnace provides a better temperature uniformity during *ex-situ* oxygen annealing. Therefore, the combination of all these features results in such immense differences in T_c , *c*-axis lattice parameters, and in-field J_c for *in-situ* and *ex-situ* oxygen annealed GdBCO thin films.

Large peaks in *c*-direction (Fig. 3) for both oxygen annealing approaches appear due to flux pinning on threading dislocations (TD) and domain walls formed by them [23]. TDs in pristine REBCO-based superconducting thin films appear during the deposition due to island-type growth of the film and misorientation present in the growth island. When such islands coalesce, they form low-angle grain boundaries, which lead to the formation of dislocation threading through the whole film [24]. In pristine REBCO thin films, the density of TDs can reach up to 10¹¹ lines/cm². In case of *ex-situ* annealed GdBCO thin films in addition to a large peak at 180°, a large shoulder between 235° and 270° appears due to competitive flux pinning at SF and Gd₂O₃ NPs [25]. Small variations of J_c across all magnetic field orientations may be caused by slow diffusion processes at 450 °C. According to our model of tailoring the defect morphology in GdBCO thin films, which will be published elsewhere, Gd₂O₃ NPs are decomposing at 450 °C and 1 bar of oxygen pressure. This NP decomposition combined with the “healing effect” during long exposure to 450 °C and 1 bar, which reduces the density of 0-dimensional defects such as oxygen vacancies, results in “shifts” of $J_c(\theta, B)$ curves in Fig. 4.

V. CONCLUSION

Pristine GdBCO superconducting thin films were *in-situ* and *ex-situ* annealed at 450 °C and 0.4 bar or 1 bar of oxygen pressure, respectively. The variation of t_{ann} between 5 and 60 min has shown that during *in-situ* oxygen annealing samples require at least 30 min of exposure to the oxygen atmosphere to achieve high in-field J_c . Compared to *in-situ*, *ex-situ* annealed GdBCO thin films have shown higher self-field and in-field J_c , which implies that J_c can be further enhanced by changing the oxygen annealing procedure, and implementation of such oxygen annealing procedure may reduce the production time of coated conductors.

ACKNOWLEDGMENT

We would like to thank P. Cayado for numerous fruitful discussion and M. Erbe for technical assistance during oxygen annealing experiments.

REFERENCES

- [1] J. P. F. Feighan et al., "Materials design for artificial pinning centers in superconductor PLD coated conductors," *Supercond. Sci. Technol.*, vol. 30, 2017, Art. no. 123001.
- [2] Y. Yamada et al., "Epitaxial nanostructure and defects effective for pinning in Y(RE)Ba₂Cu₃O_{7-x} coated conductors," *Appl. Phys. Lett.*, vol. 87, 2005, Art. no. 132502.
- [3] A. Goyal et al., "Irradiation-free, columnar defects comprised of self-assembled nanodots and nanorods resulting in strongly enhanced flux-pinning in YBa₂Cu₃O_{7-δ} films," *Supercond. Sci. Technol.*, vol. 18, 2005, Art. no. 1533.
- [4] J. L. MacManus-Driscoll et al., "Strongly enhanced current densities in superconducting coated conductors of YBa₂Cu₃O_{7-x} BaZrO₃," *Nature Mater.*, vol. 3, pp. 439–443, 2004.
- [5] B. Maiorov et al., "Synergetic combination of different types of defect to optimize pinning landscape using BaZrO₃-doped YBa₂Cu₃O₇," *Nature Mater.*, vol. 8, pp. 398–404, 2009.
- [6] I. A. Golovchanskiy et al., "Significant tunability of thin films functionalities enabled by manipulating magnetic and structural domains," *Appl. Surf. Sci.*, vol. 311, pp. 549–557, 2014.
- [7] K. Matsumoto et al., "High- J_c Gd-Ba-Cu-O epitaxial thin films prepared by pulsed laser deposition," *IEEE Trans. Appl. Supercond.*, vol. 15, no. 2, pp. 2719–2722, Jun. 2005.
- [8] H. L. Tuller and E. Opilla, "Defects and oxygen diffusion in high- T_c superconductors," *Solid State Ionics*, vol. 40/41, pp. 790–794, 1990.
- [9] J. R. LaGraff and D. A. Payne, "Concentration-dependent oxygen diffusivity in YBa₂Cu₃O_{6+x}. II. Oxygen partial pressure studies," *Phys. C: Supercond. Appl.*, vol. 212, pp. 478–486, 1993.
- [10] K. Tsuda et al., "Observation of oxygen in YBCO thin films during cooling down process using ¹⁸O tracer," *Phase. Trans.*, vol. 41, pp. 159–163, 1993.
- [11] A. Michaelis et al., "A study of oxygen diffusion in and out of YBa₂Cu₃O_{7-δ} thin films," *J. Appl. Phys.*, vol. 83, no. 12, pp. 7736–7743, 1998.
- [12] S. I. Bredikhin et al., "Anisotropy of oxygen self-diffusion in YBa₂Cu₃O_{7-δ} single crystals," *Phys. C*, vol. 179, pp. 286–290, 1991.
- [13] E. A. F. Span et al., "Oxygen diffusion in laser-ablated YBa₂Cu₃O_x thin films studied by spectroscopic ellipsometry," *Mater. Sci. Eng.*, vol. B56, pp. 123–129, 1998.
- [14] M. D. Vazquez-Navarro et al., "A study and modelling of oxygen diffusion in YBa₂Cu₃O_{7-δ} under isothermal conditions," *Supercond. Sci. Technol.*, vol. 12, pp. 1117–1122, 1999.
- [15] S. Tsukui et al., "Oxygen tracer diffusion in YBa₂Cu₃O_y superconductors," *Phys. C*, vol. 351, pp. 357–362, 2001.
- [16] Z. Mori et al., "Oxygen diffusion in c-axis oriented Y₁Ba₂Cu₃O_{7-δ} thin films," *J. Appl. Phys.*, vol. 110, 2011, Art. no. 033915.
- [17] R. J. Cava et al., "Oxygen stoichiometry, superconductivity and normal-state properties of YBa₂Cu₃O_{7-δ}," *Nature*, vol. 329, pp. 423–425, 1987.
- [18] J. L. Routbort and S. J. Rothman, "Oxygen diffusion in cuprate superconductors," *J. Appl. Phys.*, vol. 76, pp. 5615–5628, 1994.
- [19] T. B. Lindemer et al., "Experimental and thermodynamic study of non-stoichiometry in YBa₂Cu₃O_{7-x}," *J. Amer. Ceram. Soc.*, vol. 72, no. 10, pp. 1775–1788, 1989.
- [20] K. Miyachi et al., "The effect of the substitution of ga for ba site on Gd_{1+x}Ba_{2-x}Cu₃O_{6+δ} thin films," *Phys. C*, vol. 392–396, pp. 1261–1264, 2003.
- [21] J. W. Lee et al., "Stability phase diagram of GdBa₂Cu₃O_{7-δ} in low oxygen pressures," *J. Alloys Compounds*, vol. 602, pp. 78–86, 2014.
- [22] P. Cayado et al., "Untangling surface oxygen exchange effects in YBa₂Cu₃O_{6+x} thin films by electrical conductivity relaxation," *Phys. Chem. Chem. Phys.*, vol. 19, pp. 14129–14140, 2017.
- [23] V. M. Pan and A. V. Pan, "Vortex matter in superconductors," *Low Temp. Phys.*, vol. 27, pp. 732–746, 2001.
- [24] S. J. Pennycook et al., "Growth and relaxation mechanism of YBa₂Cu₃O_{7-δ} films," *Phys. C*, vol. 202, pp. 1–11, 1992.
- [25] A. K. Jha et al., "Isotropic enhancement in the critical current density of YBCO thin films incorporating nanoscale Y₂BaCuO₅ inclusions," *J. Appl. Phys.*, vol. 122, 2017, Art. no. 093905.